Journal of Statistical Physics, Vol. 37, Nos. 5/6, 1984

Further Monte Carlo Calculations for the Classical One-Component Plasma in the Range $100 \leqslant \Gamma \leqslant 160$: The FCC Lattice

H. Lawrence Helfer,[1,2] Robert L. McCrory,[2] and Hugh M. Van Horn[1,2]

Received May 17, 1984

Very accurate Monte Carlo calculations for the one-component plasma (OCP) have been compared with the results of Slattery, Doolen, and DeWitt.[1,2] We confirm their results and also find a slight dependence of the calculation of the internal energy per particle upon N, the number of particles. A detailed investigation for $N = 108$ permits us to evaluate the Helmholtz free energy for an OCP fcc lattice. As is usually believed, we find that the bcc lattice is more stable than the fcc lattice. The transition from the liquid to the fcc lattice phase occurs when $\Gamma^{\text{fcc}} = 196 \pm 1$. A three-dimensional modified cubic procedure, capable of achieving high accuracy in using tables of two-particle interaction potentials, is described in Appendix B.

KEY WORDS: One-component plasma; FCC lattice; Monte Carlo calculations.

1. INTRODUCTION

The purpose of this paper is to compare some recent Monte Carlo calculations we have performed for the OCP with the results of similar calculations which have been published recently by Slattery, Doolen, and DeWitt.[1,2] Our aim is to provide an independent check of the accuracy of the results presented in Refs. 1 and 2 and to gather further information about the anomalous N-dependent behavior found in Ref. 2 for the range $100 < \Gamma < 160$. Here, $\Gamma = (Ze)^2/akT$ is the Coulomb coupling parameter introduced in the pioneering work by Brush, Sahlin, and Teller,[3] where a is

[1] Department of Physics and Astronomy and C. E. Kenneth Mees Observatory, University of Rochester, Rochester, New York 14627.

[2] Laboratory for Laser Energetics, University of Rochester, 250 East River Road, Rochester, New York 14623.

0022-4715/84/1200-0577$03.50/0 © 1984 Plenum Publishing Corporation

822/37/5-6-6

the ion sphere radius given by $\rho = 3/(4\pi a^3)$, and ρ is the number density of particles of charge Z.

Our calculations have been carried out using a modified version of the Monte Carlo OCP code originally developed by J. P. Hansen[4] and kindly made available to us by him. Hansen's program has been employed to carry out a thorough study of the OCP during the past decade and the investigations by Hansen and his coworkers have been largely responsible for the emergence of the OCP as an important subdiscipline of statistical physics (cf. Ref. 5 and references therein).

2. BASIC METHODOLOGY

Our principal modification of Hansen's code has been to replace the optimized Kubic harmonic expansion of the interparticle pair potential employed by Hansen[4] (and improved by Slattery, Doolen, and DeWitt[1,2]) with a three-dimensional table look up, as was used by Hubbard and Slattery.[6] Our calculation thus utilizes a different method of calculation of the critical pair interaction potential from that employed in Refs. 1 and 2 and can therefore be used to check the accuracy of their results.

To compute the table of pair potentials used by our version of Hansen's OCP code, we have carried out a completely independent evaluation of the Ewald sums necessary to take into account the infinite number of periodic images of the N point charges which form the basis of the Monte Carlo computation (cf. Refs. 3 and 4).

Following Ref. 1, the total internal energy U for a classical one-component plasma (OCP) for particles interacting through a Coulomb potential is given by

$$\frac{U}{NkT} = \frac{U_0}{NkT} + \frac{1}{2} \sum_{i \neq j=1}^{N} \frac{\psi(|\mathbf{r}_i - \mathbf{r}_j|)}{NkT} \tag{1}$$

where

$$\frac{U_0}{NkT} = -1.4186487395 \frac{\Gamma}{L}, \qquad \frac{\psi(\mathbf{r})}{NkT} = \frac{\Gamma}{NL} [U_1(r) + U_2(\mathbf{r})] \tag{2}$$

and

$$U_1(r) = \frac{1}{r} \operatorname{erfc}(\sqrt{\pi}\, r) - 1 \tag{3}$$

$$U_2(\mathbf{r}) = \sum_{\mathbf{n}}{}' \frac{1}{|\mathbf{n} - \mathbf{r}|} \operatorname{erfc}(\sqrt{\pi}\, |\mathbf{n} - \mathbf{r}|) + \sum_{\mathbf{n}}{}' \frac{1}{\pi n^2} \exp(-\pi n^2) \{\exp[i(2\pi \mathbf{n} \cdot \mathbf{r})]\} \tag{4}$$

Here the distance between particles $\mathbf{r} = \mathbf{r}_i - \mathbf{r}_j$, is measured in units of La, where a is the ion sphere radius, $L = (4\pi N/3)^{1/2}$, and N is the number of particles. The vector $\mathbf{n}$ is a vector with integer components, the prime on the summation sign indicates $\mathbf{n} = (0, 0, 0)$ is excluded, and r varies between zero and unity. To evaluate the potential within the OCP Monte Carlo code [see Eqs. (3) and (4)], we used a modified cubic spline interpolation formula which has been designed to give a nearly zero mean deviation from the exact potential within each interpolation region. Details of the interpolation procedure are given in Appendix B.

Although, as Ref. 1 points out, a polynomial procedure may be more rapid for a vector computer, we chose the tabular procedure because of its flexibility for future investigations with more complicated two-body interactions. As an example, the OCP calculations could be extended to include consideration of finite temperature electron contributions. The effect of a linear zero-temperature electron response has been considered by Hubbard and Slattery.[6] The effect of finite temperature electron distributions can be developed by using a formalism for the electron density matrix such as that developed by March and Murray.[7] For a given electron temperature and Γ, new Ewald tables [similar to the tabulation of Eq. (4)] have been constructed and can be used with the present simulation code.

The Monte Carlo calculation was performed as outlined in Ref. 1. For a given Γ, the mximum step size allowed in moving ions was adjusted so that the probability of accepting new positions was 0.3–0.4. Once equilibrium was reached, the number of configurations used was sufficiently high that in principle the average ion could random walk from its initial position, using only the acceptable position changes, to a position several box lengths distant.

3. RESULTS

Our modified OCP Monte Carlo code has been used to compute the internal energies for several different values of Γ in the range from $100 \leqslant \Gamma \leqslant 160$. The results are given in Table I, together with results from Ref. 1 and 2 for the same range of Γ values. Comparison of the two sets of data shows that *our numerical results agree very well with theirs*, to within the combined limits of accuracy of our respective calculations. In most cases, the difference is less than our combined error estimates, and in no case does it exceed twice this value.

With this confirmation of the accuracy of the calculations reported in Refs. 1 and 2, we found it very striking that the results obtained in those investigations showed N-dependent differences in the computed internal energies U at a given value of Γ that frequently exceeded seven or eight times

Table I. Results of This Work Compared with Those of Ref. 1

	This calculation					Reference 1		
	N^a	U/NkT	Error	Type of start	No.[b] config's.	U/Nkt	Error	Type of start
100	256	−87.519	±0.004	liq.	3	—	—	—
125	108	−109.834	±0.005	liq.	1.7	−109.825	±0.007	liq.
125	128	−109.771	±0.003	liq.	5	−109.780	±0.004	liq.
125	128	−109.783	±0.003	lat.	2	—	—	—
125	256	−109.795	±0.003	liq.	5	—	—	—
140	108	−123.223	±0.008	lat.	1.3	−123.239	±0.010	liq.
140	128	−123.151	±0.002	liq.	2.5	−123.160	±0.006	liq.
140	128	−123.756[c]	±0.006	lat.	2	—	—	—
140	256	−123.173	±0.003	liq.	5	—	—	—
150	54	−132.33[d]	±0.01	liq.	0.3	—	—	—
150	54	−132.782	±0.006	lat.	1.2	—	—	—
150	108	−132.153	±0.005	liq.	2	—	—	—
150	108	−132.151	±0.007	liq.	1.3	—	—	—
150	108	−132.729	±0.006	lat.	1.7	—	—	—
150	118[e]	−132.127	±0.006	liq.	1.4	—	—	—
150	128	−132.075	±0.004	liq.	2.5	−132.078	±0.007	liq.
150	128	−132.750[c]	±0.007	lat.	1.0	—	—	—
150	256	−132.088	±0.003	liq.	5	—	—	—
150	500	−132.103	±0.003	liq.	10	—	—	—
155	128	−136.547	±0.004	liq.	2.5	—	—	—
160	108	−141.101	±0.009	liq.	1.3	−141.098	±0.009	liq.
160	108	−141.702	±0.005	lat.	2.6	−141.690	±0.010	lat.
160	128	−140.986	±0.004	liq.	2	−141.000	±0.006	liq.
160	128	−141.722	±0.003	lat.	1.5	−141.729	±0.006	lat.
160	256	−141.020	±0.003	liq.	5	—	—	—
160	256	−141.771[c]	±0.005	lat.	2	—	—	—

[a] Number of particles.
[b] In millions of configurations.
[c] Metastable: prior to melting.
[d] Prior to freezing.
[e] This configuration cannot freeze into a fcc or a bcc lattice.

the estimated errors. These differences appear to be real. We found the differences between the results of the calculations given in Table II of Ref. 1 for 108 particles and for 128 particles to be particularly interesting, because 128 particles freeze into a body-centered cubic (bcc) lattice, while 108 particles freeze into a face-centered cubic (fcc) lattice. In general, systems containing $N = 2I^3$ particles and their periodic images can only freeze into bcc structures, while systems containing $N = 4I^3$ particles and their images

Table II. Fits to 108-particle Monte Carlo Data

	U/NkT MC	U/NkT[a,b] fitted	Relative error
1	−0.573	-0.573_0	0.000_0
6	−4.592	-4.592_5	-0.000_5
10	−7.993	-7.991_8	0.001_2
15	−12.310	-12.307_6	0.002_4
30	−25.426	-25.432_4	-0.006_4
40	−34.251	-34.250_7	0.000_3
60	−51.961	-51.963_8	-0.002_8
80	−69.727	-69.735_1	-0.008_1
100	−87.534	-87.541_2	-0.007_2
125	−109.825	−109.831	-0.006_0
140	−123.239	-123.217_4	0.021_6
160	−141.098	-141.077_0	0.020_9
160	−141.690	−141.694	-0.003_5
180	−159.654	−159.642	0.012_3
200	−177.574	−177.581	-0.007_1
300	−267.205	−267.220	-0.015_3

[a] For $1 \leqslant \Gamma \leqslant 160$, liquid data are fitted by Eq. (5) with parameters $a = -0.89881$, $b = 1.02113$, $c = 0.28398$, and $d = -0.97930$.

[b] For $160 \leqslant \Gamma \leqslant 300$, lattice data are fitted by Eq. (6) with parameters $u_0 = -0.895873$ and $h = 3741$.

are consistent only with fcc structures, where I is a positive integer. It is easy to see that no value of N is compatible with both crystal structures, as this would require $I_{\text{bcc}} = 2^{1/3} I_{\text{fcc}}$.

As the internal energies for 108-particle calculations are significantly lower than those for the 128-particle calculations when $\Gamma > 100$, in light of the more accurate Monte Carlo data now available we decided to recheck the conclusion that the bcc lattice is always the most stable.[8,11] To accomplish this, we have followed the procedure used in Refs. 1 and 2. For the liquid data ($1 \leqslant \Gamma \leqslant 160$), we have fitted the Monte Carlo results to the expression

$$U/NkT = a\Gamma + b\Gamma^{1/4} + c\Gamma^{-1/4} + d \tag{5}$$

by minimizing the squares of the relative errors using a, b, c, and d as parameters. For the solid phase, we have fitted the results to the expression

$$U/NkT = u_0\Gamma + 3/2 + h\Gamma^{-2} \tag{6}$$

where $u_0\Gamma = -0.895873\Gamma$ (Ref. 3) is the Madelung energy of the fcc lattice and the single parameter h is obtained by minimizing the squares of the relative errors. We have checked our procedure by verifying that we reproduce the 128-particle fits given by Ref. 1. Since some of the N-dependence may be due to computational procedures, to avoid systematic errors in comparing with the 128-particle data, we have used the 108-particle data of Ref. 1 exclusively. Our results are given in Table II. The parameters obtained in our fits are quite similar to those obtained for the 128-particle data in Ref. 1.

It is worth noting that the differences between liquid, the bcc lattice, and the fcc lattice are clearly apparent in the pair correlation functions, $g(r)$. In Fig. 1, we have plotted the values of $g(r)$ from our calculations at $\Gamma = 160$ for the liquid phase in our 128-particle, liquid-start calculation; for the metastable bcc lattice phase in our 128-particle, lattice-start calculation; and for the metastable fcc lattice phase in our 108-particle, lattice-start calculation.

To determine the value of Γ at which the transition from the liquid phase to the fcc lattice phase occurs in the 108-particle data, we require the

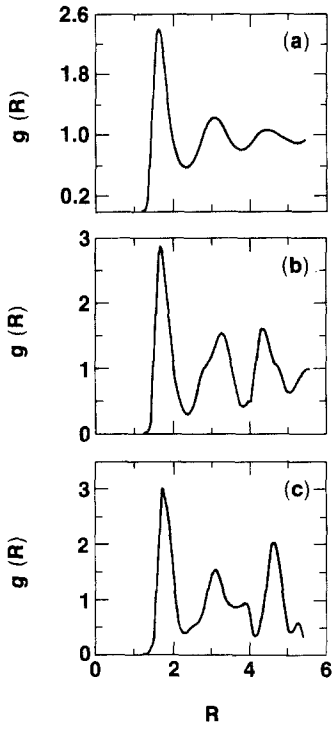

Fig. 1. Pair correlation functions for the OCP at $\Gamma = 160$. Curve (a) corresponds to 128-particle liquid state data. Curve (b) represents the (metastable) 128-particle, bcc lattice phase. Curve (c) depicts the (metastable) 108-particle fcc lattice phase. Separations are measured in units of the ion sphere radius, a.

Helmholtz free energy F for this system. These may be obtained by the methods described in Refs. 1 and 2. For the liquid phase, integration of Eq. (1) and addition of the ideal gas contribution yields

$$\frac{F(\Gamma)}{NkT} = \int_0^\Gamma \frac{U(\Gamma')}{NkT}\frac{d\Gamma'}{\Gamma'} = b\Gamma + 4(b\Gamma^{1/4} - c\Gamma^{-1/4}) + (d+3)\ln\Gamma - [a + 4(b-c) + 1.1516] \tag{7}$$

as given in Ref. 2. For the fcc lattice phase, we write the free energy as the sum of the anharmonic approximation plus the harmonic contribution represented by the final term in Eq. (2). From Refs. 3 and 1 we thus have

$$\frac{F}{NkT} = \frac{F_0}{NkT} + \frac{1}{N}\sum_{j=1}^{3N-3} \ln\frac{\omega_j}{\omega_p} + 3\ln\frac{h\omega_p}{kT} - \frac{h}{2\Gamma^2} \tag{8}$$

where F_0 represents the Madelung energy, and ω_p in the ion plasma frequency. We have evaluated the fcc lattice vibration frequencies as described in Appendix A and have written the lattice free energy in the form

$$\frac{F}{NkT} = -0.895873\,\Gamma + \frac{9}{2}\ln\Gamma - 1.8856 - \frac{h}{2\Gamma^2} + \frac{1}{N}\sum_{j=1}^{3N-3}(\ln\omega_j^{\text{fcc}} - \ln\omega_j^{\text{bcc}}) \tag{9}$$

We have chosen this form to minimize the effects of inaccuracies in the summation over the lattice vibration frequencies. We obtain

$$\frac{1}{N}\sum_{j=1}^{3N-3}(\ln\omega_j^{\text{fcc}} - \ln\omega_j^{\text{bcc}}) = -0.799_5 + 0.850_7 \tag{10}$$

yielding

$$\frac{F}{NkT} = -0.895873\Gamma + \frac{9}{2}\ln\Gamma - 1.834_4 - \frac{1}{2}0.3741\Gamma^{-2} \tag{11}$$

When Eq. (11) for the fcc lattice free energy is combined with Eq. (7) for the liquid phase free energy, we find the value of Γ at the phase transition to be

$$\Gamma_m^{\text{fcc}} = 196 \pm 1 \tag{12}$$

The quoted uncertainty corresponds to an error of ± 0.005 in U/NkT, which is approximately our estimated error. The corresponding value for the tran-

sition from the liquid to the bcc lattice phase is $\Gamma_m = 178 \pm 1$ (Ref. 2). Thus, the transition to the bcc phase occurs prior to the postulated transition to the fcc phase in a cooling sequence (increasing Γ). Further, direct comparison of the free energy of the fcc lattice given by Eq. (11) with that of the bcc lattice given by Refs. 1 and 2 shows that the free energy of the bcc lattice remains lower than that of the fcc lattice for all larger values of Γ.

4. CONCLUSION

We have confirmed the conclusion that the bcc lattice is more stable than the fcc, with the more accurate Monte Carlo data now available. The dependence of the internal energy, U/NkT, on N appears very complicated and not as simple as that discussed in Slattery *et al.* (Ref. 2). For $\Gamma < 160$, the 500-particle calculations clearly give lower U/NkT than the 128-particle calculations; however, so do the 108-particle calculations. Also, we do not find strong evidence for the "bump" in the curve of U/NkT vs. Γ for the range $\Gamma = 140$–160 which the authors of Ref. 2 thought present. Further understanding of the classical OCP must await interpretation of the N dependence of the results. The modified three-dimensional spline procedure for determining the two-particle interaction potentials accurately has been thoroughly tested and may be used in a variety of other statistical mechanics problems.

ACKNOWLEDGMENT

We are grateful to J. P. Hansen for providing us with a copy of his Monte Carlo OCP code. The authors gratefully acknowledge the technical assistance of Mr. Bruce Loftis and others of the staffs at the CDC Center for Applied Vector Technology and the Colorado State University in helping to modify the OCP code for efficient use of the Cyber 205 computer. The calculations reported here have been carried out in part on the Cyber 175 at the University of Rochester's Laboratory for Laser Energetics, in part on the Cyber 205 at Colorado State University, and in part on an Apple II^+-microcomputer. This work has been supported in part by the National Science Foundation under Grant No. AST 83-07214, a grant from the Center for Naval Analysis through the University of Rochester, a grant from Control Data Corporation (CDC Research grant 82CSU07), and a grant from the Colorado State University.

APPENDIX A

The lattice vibration frequencies for an fcc lattice can be evaluated in the same manner as employed by Carr (Ref. 9) for the bcc lattice. In both

cases, the eigenfrequencies are the solution of the characteristic equation (Eq. 22, Ref. 9),

$$\det(G_{\alpha\beta}(\mathbf{f}) - \omega^2(\mathbf{f})\,\delta_{\alpha\beta}) = 0 \tag{A1}$$

where $\mathbf{f}$ is a vector in the unit cell of reciprocal space. Because the Eq. (A1) is third order in ω^2, there are three independent solutions for each $\mathbf{f}$. The matrix $G_{\alpha\beta}$ is given by (Eq. 21, Ref. 9)

$$G_{\alpha\beta}(\mathbf{f}) = \frac{\delta_{\alpha\beta}}{r_s^3} + G_{\alpha\beta}'(\mathbf{f}) \tag{A2}$$

where the number density of particles is given by

$$\rho = \frac{3}{4\pi}(r_s a_0)^{-3} \tag{A3}$$

and a_0 is the ionic Bohr radius. (This defines $r_s = a/a_0$, where a is the ion sphere radius.) Also from Ref. 9, Eqs. (13)–(16) and (21), we have

$$G_{\alpha\beta}'(\mathbf{f}) = \frac{3}{\pi r_s^3}\delta_{\alpha\beta}\sum_j{}' \frac{1}{|\mathbf{n}_j|^3} e^{i\mathbf{f}\cdot\mathbf{n}_j} - \frac{9}{\pi r_s^3}\sum_j{}' \frac{n_j^\alpha n_j^\beta}{|\mathbf{n}_j|^5} e^{i\mathbf{f}\cdot\mathbf{n}_j} \tag{A4}$$

where the prime denotes exclusion of the point $\mathbf{n} = (0, 0, 0)$. Here the $\mathbf{n}_j$ are normalized lattice points of a fcc lattice, which are given by

$$\mathbf{n}_j = \mathbf{R}_j/[(\pi/3)^{1/3} r_s a_0] \tag{A5}$$

The summations over lattice sites have been evaluated by Cohen and Keffer (Ref. 10), who define

$$S_3 \equiv 4\sum_j{}' \frac{1}{|\mathbf{n}_j|^3} e^{i\mathbf{f}\cdot\mathbf{n}_j} \tag{A6}$$

and

$$S_5^{\alpha\beta} \equiv 4\sum_j{}' \frac{n_j^\alpha n_j^\beta}{|\mathbf{n}_j|^5} e^{i\mathbf{f}\cdot\mathbf{n}_j} \tag{A7}$$

We have solved the eigenvalue equation (A1) using the values of S_3 and $S_5^{\alpha\beta}$ tabulated in Ref. 10, and out results are listed in Table A1. From these data, we have also computed the average of $\omega(\mathbf{k})$, which gives the zero-point

Table A1. Values for $\omega_s(\vec{f})$ and the Integration Weights $W_s(\vec{f})$ at the Points, $\vec{f}$, of the Reciprocal Lattice for which Data is Tabulated in Ref. 10.[a]

$\frac{8.2^{1/3}}{\pi}\vec{f}$	$W(\vec{f})$	$\omega_1(\vec{f})$	$\omega_2(\vec{f})$	$\omega_3(\vec{f})$	$\frac{8.2^{1/3}}{\pi}\vec{f}$	$W(\vec{f})$	$\omega_1(\vec{f})$	$\omega_2(\vec{f})$	$\omega_3(\vec{f})$
(000)	1	$3^{1/2}$	0	0	(5.31)	48	1.480	0.761_9	0.478_5
(111)	8	1.720	0.141_4	0.141_4	(533)	24	1.575	0.577_1	0.432_3
(200)	6	1.693	0.259_4	0.259_4	(551)	24	1.366	0.946_6	0.489_0
(220)	12	1.682	0.386_8	0.151_2	(600)	6	1.478	0.638_5	0.638_5
(222)	8	1.692	0.262_6	0.262_6	(620)	24	1.421	0.762_1	0.632_9
(311)	24	1.654	0.359_4	0.367_8	(622)	24	1.424	0.815_8	0.554_5
(331)	24	1.623	0.542_9	0.266_2	(640)	24	1.271	1.016	0.592_0
(333)	8	1.663	0.342_3	0.342_3	(642)	24	1.430	0.827_0	0.520_3
(400)	6	1.591	0.483_6	0.483_6	(660)	4	1.241	1.048	0.599_8
(420)	24	1.577	0.599_2	0.393_6	(711)	24	1.398	0.783_8	0.656_4
(422)	24	1.608	0.477_9	0.430_9	(731)	48	1.269	0.972_4	0.666_9
(440)	12	1.476	0.824_7	0.376_2	(800)	3	1.426	0.694_9	0.694_9
(442)	24	1.579	0.605_8	0.373_3	(820)	12	1.330	0.822_5	0.743_9
(444)	4	1.651	0.370_1	0.370_1	(822)	8	1.241	1.048	0.599_8
(511)	24	1.521	0.617_4	0.553_2	(840)	6	1.090	1.090	0.789_8

[a] The values given for are multiplied by $r_s^{3/2}$, and 2ω is the value of the vibrational energy in ionic Rydberg units.

energy of the lattice, and the average of $\ln \omega(\mathbf{k})$, which is needed in the text. These quantities, computed by the method given in Ref. 10, are

$$\langle \omega_s(\mathbf{f}) \rangle = \frac{1}{512} \sum_{s,f\neq 0} W(\mathbf{f})\, \omega_s(\mathbf{f}) = \begin{cases} 2.650_3, & \text{bcc lattice} \\ 2.662_6, & \text{fcc lattice} \end{cases} \tag{A8}$$

$$\langle \ln \omega_s(\mathbf{f}) \rangle = \frac{1}{512} \sum_{s,f\neq 0} W(\mathbf{f}) \ln \omega_s(\mathbf{f}) = \begin{cases} -0.850_7, & \text{bcc lattice} \\ -0.799_5, & \text{fcc lattice} \end{cases} \tag{A9}$$

APPENDIX B

Rather than follow the conventional approach to expand a function $f(x, y, z)$ as a tensor product of one-dimensional cubic splines (which results in a ninth order polynomial for a three-dimensional problem), we chose instead to use the form

$$f(x, y, z) = \sum_{i,j,k=1}^{2} \delta x_i\, \delta y_i\, \delta z_k [f(2-i, 2-j, 2-k) + \Delta x_i f_{xx}(2-i, 2-j, 2-k) + \Delta y_j f_{yy}(2-i, 2-j, 2-k) + \Delta z_k f_{zz}(2-i, 2-j, 2-k)] \tag{1}$$

where the interpolation cell is a unit cube, and

$$\delta x_1 = x - x_0 \qquad \delta x_2 = 1 - \delta x_1$$
$$\Delta x_1 = \delta x_1^2 - 1 \qquad \Delta x_2 = \delta x_2^2 - 1$$

and similar definitions hold for δy_j, δz_k, Δy_j, and Δz_k. Here (x_i, y_j, z_k) are the coordinates of the tablulated values of f. For each triplet (x, y, z), tabular values of f and f_{xx}, f_{yy}, and f_{zz} at the eight corners of the cube containing (x, y, z), are indicated by $f(i, j, k)$ and $f_{xx,yy,zz}(i, j, k)$ where $i, j, k = 0$ or 1. Note that Eq. (1) is the usual trilinear form if the second derivatives, f_{xx}, f_{yy}, f_{zz}, are removed. If two coordinates are held fixed, Eq. (B1) is of the same form as a standard cubic spline. The function f (and its associated second derivatives) enables us to determine ψ in Eq. (1) using $\psi(\mathbf{r}) = f(\mathbf{r}) + 1/r$. The motivation for this procedure is twofold: (1) the form of Eq. (B1) assures that for potential functions f, the source term [obtained by constructing $\nabla^2 f$ from Eq. (1)] varies linearly in an interpolation cell and is piecewise continuous (the procedure only requires four functions $f, f_{xx}, f_{yy}, f_{zz}$ to be tabulated); and (2) because we are effectively evaluating second derivatives, removing the $1/r$ variation of the tabulated function results in a function whose second derivatives are not large at $r = 0$.

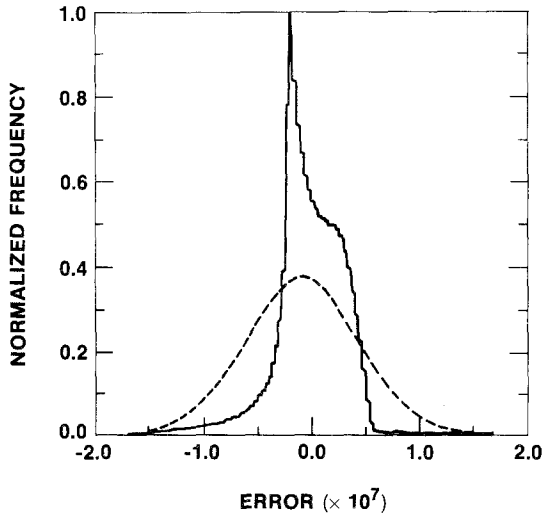

Fig. 2. Histogram of the differences Eq. (1) – Eq. (B1), "true" minus interpolated values of the pair potential for 500,000 randomly chosen sets of interparticle coordinate distances. The true potentials are accurate to one part in 10^9. The +++ curve is a Gaussian with the same mean, variance, and area as the histogram. The maximum observed error was $< 2 \times 10^{-7}$.

Taking advantage of the cubic symmetry of Eq. (4), storage is reduced by ordering ($z \geqslant y \geqslant x$) the tabular values of f. We have used 40 knots ($0 < (x, y, z) < 0.5$) in each dimension in the construction of our tables for f. In Fig. 2, we show the results of our procedure, obtained by evaluating the potential, calculated from Eq. (4), for 500,000 random positions and comparing the results with Eq. (B1). The maximum error introduced by our procedure never exceeds one part of 10^7, and the mean and standard deviation for all the trials was -8.6×10^{-9} and 5.1×10^{-8}, respectively. (If the cubic terms are omitted in Eq. (B1), the accuracy is decreased by a factor of 100.) The mean should be compared with the mean value obtained by Ref. 1, 6.5×10^{-8} and the deviation with their values, 4.9×10^{-8}. Thus, our accuracy is at least that used in Ref. 1; however, our *maximum* error is 10^3 times smaller than theirs.

REFERENCES

1. W. L. Slattery, G. D. Doolen, and H. E. DeWitt, *Phys. Rev.* **A21**:2087 (1980).
2. W. L. Slattery, G. D. Doolen, and H. E. DeWitt, *Phys. Rev.* **A26**:2255 (1982).
3. S. G. Brush, H. L. Sahlin, and E. Teller, *J. Chem. Phys.***45**:2102 (1966).
4. J. P. Hansen, *Phys. Rev.* **A8**:3096 (1973).
5. M. Baus and J. P. Hansen, *J. Stat. Phys.* **31**:409 (1983).
6. W. B. Hubbard and W. L. Slattery, *Astrophys. J.* **168**:131 (1971).
7. N. March and A. Murray, *Phys. Rev. A* **120**:830 (1961); *Proc. R. Soc. London Ser.* **A261**:119 (1961).
8. E. L. Pollack and J. P. Hansen, *Phys. Rev.* **A8**:3110 (1973).
9. W. J. Carr, Jr., *Phys. Rev.* **122**:1437 (1961).
10. M. H. Cohen and F. Keffer, *Phys. Rev.* **99**:1128 (1955).
11. A. D. J. Haymet, *Phys. Rev. Lett.* **52**:1013 (1984).